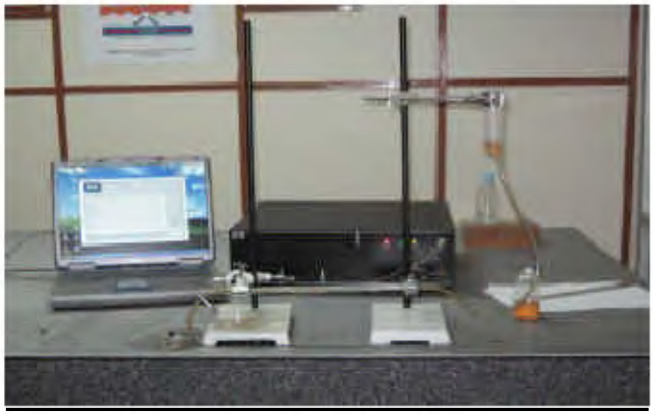

Figure 3. Experimental set-up for petrol leak detection.

ately. A Bragg wavelength shift of 0.2 nm is recorded even for this short duration of petrol leak, which can be improved easily either by increasing the petrol contact time or by manipulating the size of the rubber tube. The experiment has been performed repeatedly in a controlled laboratory environment where the timing and extent of petrol leak is controlled manually, but this sensor should work equally well in actual field applications (Figure 3). The properties of transducer rubber tube do not change after repeated (up to ten times) use.

Since the sensed information, namely petrol leakage, is wavelength-encoded, it is independent of fluctuations in the light source, connector or fibre losses, etc. Another point which is crucial in hazardous environment is the feasibility of remote sensing. It is because the commercial fibres have low loss in the operating wavelength range used in this study and are able to transmit the sensed information to distant monitoring locations. Besides, the narrow bandwidth of FBG allows multiplexing of many sensing elements with known Bragg wavelengths and predetermined positions along the length of the pipeline or tank by design, which works independently without interfering with each other, thereby providing distributed sensing of both leakage and its locations. This study offers an efficient, fast, safe and inexpensive technique for applications involving remote monitoring of leakage and/or spillage along with its exact location in petrol pipelines and storage tanks and can be utilized as an alarm system for the same.

1. Meltz, G., Morey, W. W. and Glen, W. H., Formation of Bragg gratings in optical fibres by a transverse holographic method. *Opt. Lett.*, 1989, **14**, 823–825.
2. Zhou, Z. *et al.*, Techniques of advanced FBG sensors: Fabrication, demodulation, encapsulation and their application in the structural health monitoring of bridges. *Pac. Sci. Rev.*, 2003, **5**, 116.
3. Ecke, W., Fiber optic sensor network for spacecraft health monitoring, *Meas. Sci. Technol.*, 2001, **12**, 974.
4. Rao, Y. J., Recent progress in applications of in-fibre Bragg grating sensors. *Opt. Lasers Eng.*, 1999, **31**, 297–324.
5. Kashyap Raman, *Fiber Bragg Gratings*, Academic Press, London, 1999.
6. Spirin V. V., Shlyagin, M. G., Miridonov, S. V., Jimenez, F. J. M. and Gutierrez, R. M. L., Fibre Bragg grating sensor for petroleum hydrocarbon leak detection. *Opt. Lasers Eng.*, 2000, **32**, 497–503.
7. Kersey, A. D. *et al.*, Fiber grating sensors. *J. Lightwave Technol.*, 1997, **15**, 1442–1463.

ACKNOWLEDGEMENTS. We acknowledge financial support from the National Programme on Smart Materials (NPSM), Govt of India and the Council of Scientific and Industrial Research (CSIR), New Delhi.

Received 16 August 2005; accepted 18 November 2005

Laser ablation-inductively coupled plasma mass spectrometry for 2D mapping of trace elements in soft tissues

N. Chandra Sekaran

GIFU University, River Basin Research Center, Yanagido, GIFU, 501-1193, Japan

Metals are not homogeneously distributed in organ tissues. Although most mapping techniques, such as histologic staining methods, have been developed for element imaging on subcellular level, many suffer from either low precision or poor detection limits. Therefore, small variations in elemental distribution cannot be identified. We have developed a method using laser ablation-inductively coupled plasma mass spectrometry for the determination of elemental distribution in lamb liver using 2D mapping.

Keywords: Copper zonation, CRM pig liver paste, LA–ICP–MS, mapping, soft tissues.

LASER ablation has been used in the determination of trace elements in different non-biological solid samples like glass[1], geological materials[2], metal sheets[3], polymers[4], and even ice cores[5]. Although there have been a few studies on biological samples, all of them were hard tissues like tree rings[6–9], tree barks[10], teeth[11,12], leaves[13] and shells from bivalves[14–17]. Limited information is available about the applicability of a laser ablation system for fresh soft tissues like liver or brain.

In biological and clinical applications, it is often desirable to acquire knowledge about the distribution of a trace element in a soft tissue. Regional localization of trace elements in a thin section of lamb liver can be identified

e-mail: Natarajan@green.gifu-u.ac.jp

using 2D mapping. Moreover, zones of accumulation of trace elements can be determined in a thin section of lamb liver tissue. This technique could improve our knowledge of how trace elements are distributed in tissues on a micro to millimetre scale.

Traditionally, pathologists have used staining methods for the different elements of interest. These methods have disadvantages: they are often not sensitive enough to detect trace and ultratrace concentrations of elements, or the chemicals used for staining introduce impurities[18]. Although these methods are element-specific, this is a disadvantage if more than one element has to be mapped in the tissue. In addition, some of the chemical reactions are metal species-specific. For example, complexing agents must compete with cysteine-rich proteins (metallothioneins) to bind the metal. Thus, staining methods such as the rhodamine method for copper can identify free copper, but not the copper bound in copper proteins[19]. Other methods, such as scanning nuclear microprobes[18], microPIXE[20], secondary ion mass spectrometry[21,22], laser microprobe mass analysis[23], energy-dispersive X-ray analysis[24–26], and electron probe X-ray microanalysis[27], suffer from either low precision or poor detection limits. Laser microprobe mass analysis, however, is an ideal technique for the determination of trace element distribution in biological samples. It is a rather sensitive tool, with detection limits in the upper ppm range (1–100 μg/g). However, because the ionization of elements is strongly dependent on the matrix and therefore rather difficult to calibrate, this technique can be considered only as a qualitative method. Furthermore, the thin sections should not be thicker than 2 μm, which makes sample preparation rather difficult[23].

LA–ICP–MS method offers the possibility of producing spatial information on element distribution at micrometre scale in solid materials[20]. Recent developments in matrix-assisted laser desorption–ionization time-of-flight mass spectrometry allow a spatial resolution of 30 μm for direct mapping of compounds in the mass range between 1 and 50 kDa in tissue sections[21,28]. However, when an LA system is coupled to an inductively coupled plasma mass spectrometer (ICP–MS), the ablated material is fully ionized in the argon plasma and elements are detected by an element-specific detector[29].

The present study envisages the applicability of laser ablation towards 2D mapping for trace elements in lamb liver (New Zealand, NZ) section. Trace element availability in bulk tissue, indicates total concentration of the element

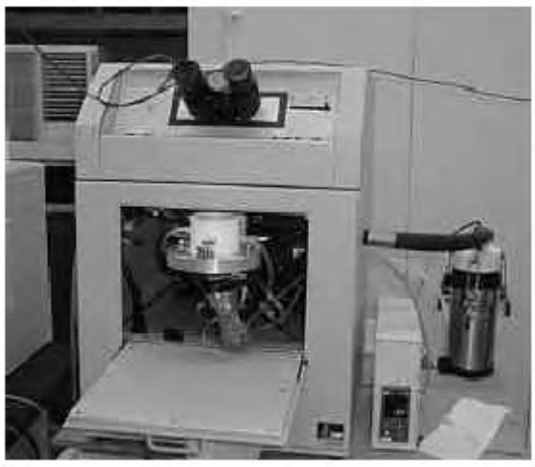

Figure 1. Laser ablation with cryogenically cooled ablation system.

Figure 2. 3 × 3 Raster points on NZ lamb liver section (30 μm) showing lobular bodies. Laser parameters were 1 burst, 200 μm spot size, 6.5 mJ.

Table 1. Reproducibility of the signal. Influence of ablation cell temperature on reproducibility of laser signal using lamb liver sample (n = 15). LA conditions: 100% power, 20 Hz, 200 μm spot size, 50 shots

	Reproducibility (%)			
Isotope	–20°C	–40°C	–60°C	–80°C
^{13}C	18.2	10.9	5.8	4.1
^{68}Zn	4.2	3.8	2.6	2.6
^{98}Mo	22.5	9.8	6.4	6.5

Table 2. Optimized conditions of LA–ICP–TOF–MS using cryogenically cooled ablation cell

ICP–TOF–MS parameters	Renaissance, LECO
Forward power (40.68 MHz)	1400 W
Plasma flow	14.2 l min^{-1}
Auxiliary flow	0.67 l min^{-1}
Carrier gas (Ar) flow	1.12 l min^{-1}
Integration time	1 s
Measured mass	^{12}C, ^{63}Cu, ^{64}Cu, ^{64}Zn, ^{66}Zn and ^{68}Zn
International standard	^{12}C
Laser ablation parameters	LSX 200 plus, CETAC
Laser	ND-YAG
Wavelength	266 nm
Laser energy	6.5 mJ (100%)
Focus	Sample surface
Fire frequency	10 Hz
Spot size	25–200 μm
Cryo cell temperature	–80°C

Table 3. Validation of the method (accuracy). Results of calibration function using four different fresh soft tissue samples and its validation with CRM pig liver (LGC-7112), five spot of 200 μm

	Cd (mg/kg)	Cu (mg/kg)	Zn (mg/kg)	Mo (mg/kg)
NZ lamb liver	0.063	6.87	42.4	1.25
NZ lamb kidney	0.094	102.0	39.9	1.89
Pig kidney	0.822	9.21	21.4	0.97
NR sheep kidney	16.9	5.19	39.3	0.44
Slope[#]	217.73* cts	0.5993* mV	0.4825* mV	1318.8* cts
R^2	0.999	0.986	0.998	0.993
CRM pig liver (LGC-7112) (measured)	0.31 ± 0.02	101 ± 6	43.0 ± 1.7	1.8 ± 0.1
Certified	0.25 ± 0.04	117 ± 8	43.0 ± 2.7	~1[#]
Detection limits*	0.015	0.05	0.02	~0.01

*Zn and Cu are in mV, lower R^2 reflects degree of homogeneity.
[#]Indicative.

in the tissue concerned, but it is difficult to localize trace elements in the tissues. Therefore, this technique was adopted to explore the possibility to determine the elemental distribution and to map its specific localization and quantify it using certified reference material (CRM) pig liver paste (LG-7112).

UV Nd–YAG laser with an excitation wavelength of 266 nm was used (CETAC LSX-200 Plus and DigiLaz software) with a cryogenically cooled ablation cell, which was coupled to ICP–MS (Renaissance, LECO; Figure 1). Frozen liver tissue from NZ lamb was sliced to 1 mm and used for laser ablation. Different laser parameters were provided for efficient ablation processes. Localization of trace elements for mapping was done using a thin tissue section and carried out using a cryotome –25°C. A small portion of NZ lamb liver was positioned onto the cryotome block holder and sectioned to obtain thickness of a 30 μm. It was affixed to a clean glass slide and air-dried for few minutes and introduced into the ablation chamber. The image of the liver section was captured onto the screen with the help of a CCD camera fitted to the laser system (Figure 2).

A cryogenically cooled ablation cell enables direct analysis of thin sections from fresh soft tissue samples such as liver for trace elements using laser ablation ICP–MS. Reproducibilities of about 2–6% can be achieved if the tissue samples can be ablated at a temperature below –60°C (Table 1). Variation of cell temperature shows the benefit of using a low temperature when tissue samples are ablated. The three selected elements showed the same trend; large variation at –20°C, while below –60°C, the reproducibility was good. Moreover, during the ablation of wet tissue water enters the plasma (wet plasma) and this will affect sensitivity and signal shift. Therefore, cryogenic ablation chamber is advantageous in this application.

All laser ablation parameters were optimized (Table 2). The reproducibility of the laser signal is shown in Table 1 and the variation of raster spot size to intensity is given in Figure 2. The amount of ablated material is related to spot size, and has direct influence on signal intensity. Smaller spot size shows occurrence of a detectable signal and is of little use if distribution of the element in the tissue is the focus of the investigation. The size used therefore depends on the concentration of the element of interest and the achievable resolution if a tissue is going to be mapped.

A calibration method using three different tissue samples has been validated with CRM pig liver (LGC-7112). Good recoveries (86–124% for certified values) were achieved for Cu (100.9 mg/kg; 117 ± 8 certified), Zn, Cd, Mo (Table 3) using carbon signal as internal standard. Therefore, this CRM can be used for the quantification of other tissues with similar carbon content using a one-point calibration. Detection limits in the lower mg/kg range (Zn: 20 mg/kg) were determined based on 3σ of the blank signal with a spatial resolution of less than 200 mm. Figure 3 *a–c* shows the homogeneity in copper found in CRM material compared to the real sample, NZ lamb liver. On the other hand, zinc shows homogeneity in both CRM and the real sample. The distribution of copper is heterogeneous in NZ lamb liver.

LA coupled to ICP–MS with a cryogenically cooled ablation chamber is the ideal technique for 2D mapping of trace elements in soft tissues. Depending on the concentration of the element present, it may be possible to determine trace elements directly in tissue samples at a spatial resolution of <20 μm. This technique can be extrapolated to map specific locations of the element concerned, within an area of 100 μm in a microtomic section. LA–ICP–MS is therefore an excellent tool for histologists and molecular cell biologists to correlate certain features in tissues with multi-element distribution of trace elements in the tissues. The LA–ICP–MS technique reveals where a metal-containing drug accumulates, as in chemotherapy, or whether implants release metals into the adjacent tissue. It may be possible to compare diseased organs with healthy ones and identify differences in their trace element distributions. Trace elemental distribution pattern could be mapped for cancerous tissues and compared with non-cancerous tissues. This could lead to further investigations into the cause of prion diseases, such as bovine spongiform encephalitis, Creutzfeldt–Jakob disease, or scrapie. LA–ICP–TOF–MS has a detection limit in the lower μg kg^{-1}

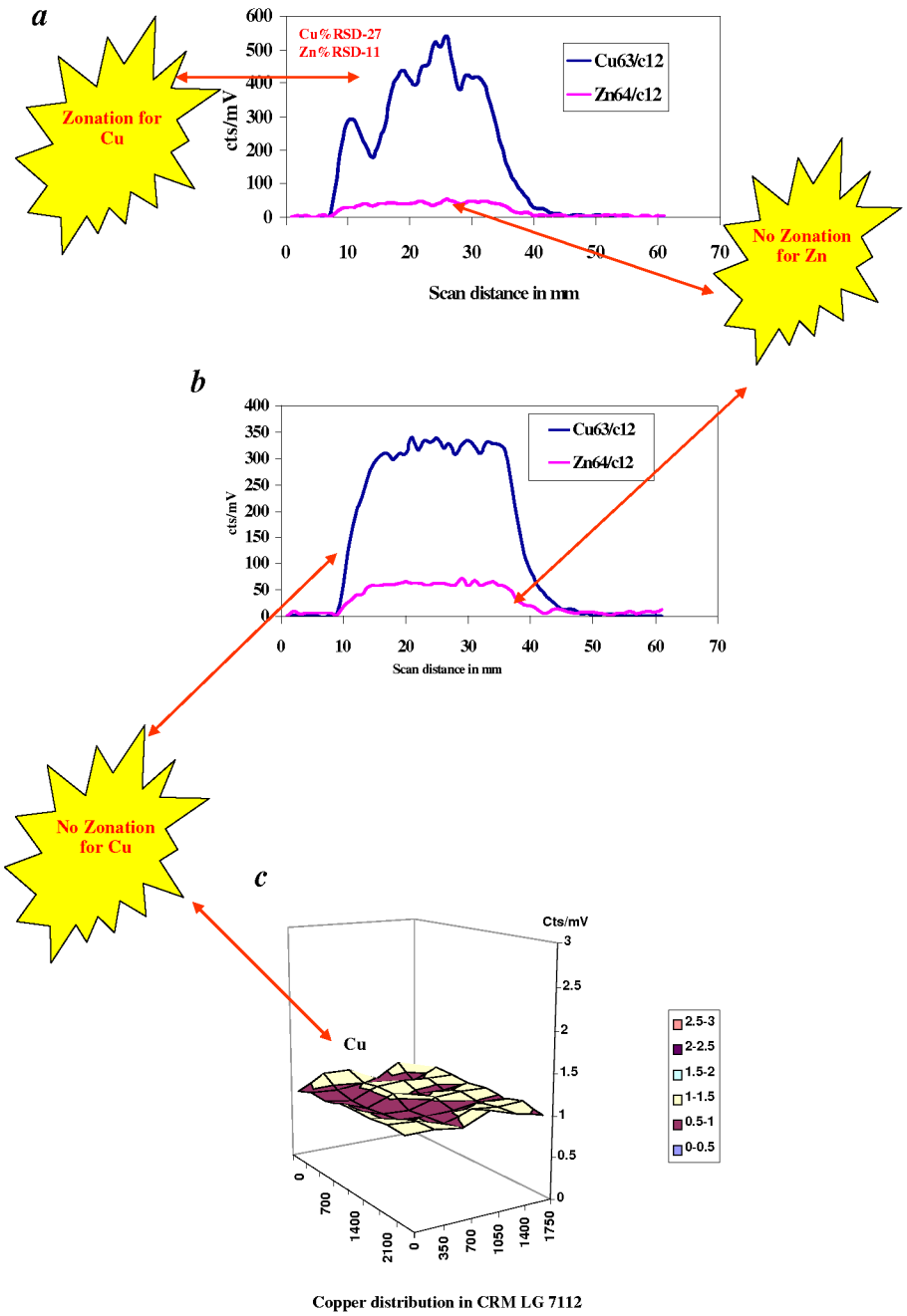

Figure 3*a–c*. ***a***, Single line scan of thin section (NZ lamb liver section). ***b***, Single line scan of a homogenized tissue CRM LG-7112 pig liver paste. Laser parameters were 100%, 10 Hz, 25 µm spot size, scan speed of 100 µm/s for (***a***) and (***b***). ***c***, Raster scan of homogenized CRM pig liver paste (LG-7112). Laser parameters were 10 Hz, 7 × 6 rasters, 200 µm spot size, 5 bursts.

range. Accuracy is satisfactorily worth using 'C' as internal standard. Precision is good enough to recognize zonation of elements in the tissue. Therefore, this technique can be used for various applications, e.g. to study metal particle distribution in the lungs of workers in occupational exposure, mapping of proteins by overlaying with elemental maps, histopathological conditions caused due to metal intoxication, distribution of copper (e.g. in prion diseases) in the hippocampus region of the brain section. Our group is now working towards trace element mapping in the hippocampus region of scrapie-infected mice brain.

1. Raith, A., Godfey, J. and Hutton, R. C., *Fresenius' Z. Anal. Chem.*, 1996, **354**, 789–792.
2. Jarvis, K. E. and William, J. G., *Chem. Geol.*, 1993, **106**, 251.
3. Huang, Y., Shibata, Y. and Morita, M., *Anal. Chem.*, 1993, **65**, 2999–3003.

4. Dobney, A. M., Mank, A. J. G., Grobecker, K. H., Conneely, P. and De Koster, C. G., *Anal. Chim. Acta*, 2000, **423**, 9.
5. Reinhardt, H., Kriews, M., Miller, H., Schrems, O., Ludke., C., Hoffmann, E. and Skole, J., *Fresenius' Z. Anal. Chem.*, 2001, **370**, 629.
6. GarbeSchonberg, C. D., Reimann, C. and Pavlov, V. A., *Environ. Geol.*, 1997, **32**, 9.
7. Watmough, S. A., Hutchinson, T. C. and Evans, R. D., *Environ. Sci. Technol.*, 1998, **32**, 2185.
8. Hoffmann, E., Lutdke, C., Scholze, H. and Stephanowitz, H., *Fresenius' Z. Anal. Chem.*, 1994, **350**, 253.
9. Watmough, S. A., Hutchinson, T. C. and Evans, R. D., *J. Environ. Qual.*, 1998, **27**, 1087,
10. Narewski, U., Werner, G., Schulz, H. and Vogt, C., *Fresenius' Z. Anal. Chem.*, 2000, **366**, 167.
11. Lee, K. M., Appleton, J., Cooke, M., Keenan, F. and Sawicka-Kapusta, K., *Anal. Chim. Acta*, 1999, **395**, 179.
12. Lochner, F., Appleton, J., Keenan, F. and Cooke, M., *Anal. Chim. Acta*, 1999, **401**, 299.
13. Hoffmann, E., Lüdke, C., Skole, J., Stephanowitz, H., Ullrich, E. and Colditz, D., *Fresenius' Z. Anal. Chem.*, 2000, **367**, 579.
14. Price, G. D. and Pearce, N. J. G., *Mar. Poll. Bull.*, 1997, **34**, 1025.
15. Bellotto, V. R. and Miekeley, N., *Fresenius Z. Anal. Chem.*, 2000, **367**, 635.
16. Toland, H., Perkins, B., Pearce, N., Keenan, F. and Leng, M. J., *J. Anal. At. Spectrom.*, 2000, **15**, 1143.
17. Richardson, C. A., Chenery, S. R. N. and Cook, J. M., *Mar. Ecol. Prog. Ser.*, 2001, **211**, 157.
18. Watt, F., *Cell Mol. Biol.*, 1996, **42**, 17–26.
19. Fuentealba, I. C., Haywood, S. and Trafford, J., *Liver*, 1987, **7**, 277–282.
20. Pearce, N. J., Perkins, W. T., Abell, I., Duller, G. A. T. and Fuge, R., *J. Anal. At. Spectrom.*, 1992, **7**, 53–57.
21. Todd, P. J., Schaaf, T. G., Chaurand, P. and Caprioli, R. M., *J. Mass Spectrom.*, 2001, **36**, 355–369.
22. Chandra, S. and Morrison, G. H., *Int. J. Mass Spectrom. Ion Process.*, 1995, **143**, 161–176.
23. Lancu, T. C. *et al.*, *Biometals*, 1996, **9**, 57–65.
24. Kupper, H., Lombi, E., Zhao, F. J., Wieshammer, G. and McGrath, S. P., *J. Exp. Bot.*, 2001, **52**, 2291–2300.
25. Ylanen, H. O., Ekholm, C., Beliaev, N., Karisson, K. H. and Aro, H. T., *Key Eng. Mater.*, 2000, **192**, 613–616.
26. Centeno, J. A. and Johnson, F. B., *Appl. Spectrosc.*, 1993, **47**, 343–345.
27. Mizuhira, V., Hasegawa, H. and Notoya, M., *Acta Histochem. Cytochem.*, 1997, **30**, 277–301.
28. Chaurand, P. and Caprioli, R. M., *Electrophoresis*, 2002, **23**, 3125–3135.
29. Günther, D., Jackson, S. E. and Longerich, H. P., *Spectrochim. Acta B*, 1999, **54**, 381–409.

Received 28 February 2005; revised accepted 7 November 2005

Status of medicinal plants in the disturbed and the undisturbed sacred forests of Meghalaya, northeast India: population structure and regeneration efficacy of some important species

R. C. Laloo, L. Kharlukhi, S. Jeeva and B. P. Mishra*

Department of Botany, School of Life Sciences,
North-Eastern Hill University, Shillong 793 022, India

Plants used by indigenous people as traditional medicine were identified from a disturbed (Swer) and undisturbed (Mairang) sacred grove of Meghalaya. Medicinal flora of the two sacred groves consists of 80 woody species. Species richness was adversely affected by anthropogenic activities and it decreased from 57 in the undisturbed to 41 in the disturbed sacred grove. Distribution of important value index was more among species in the Mairang sacred grove. The position of common species was changed from undisturbed to disturbed forests. The population structure and regeneration potential of *Camellia caduca* (endemic and less frequent), *Cinnamomum pauciflorum* (endemic and rare), *Erithroxylum kunthianum* (endemic) and *Picrasma javanica* (rare) were studied. Seedling recruitment of all four species was higher in the disturbed condition. However, per cent conversion of seedlings into saplings was more in the undisturbed forest, except in the case of *E. kunthianum*. The gaps facilitated per cent conversion of saplings into trees in the first three species. Regeneration efficiency of these species was higher in the Swer than the Mairang sacred grove.

Keywords: Anthropogenic disturbance, population structure, regeneration efficacy, sacred groves, traditional healthcare system.

PLANTS have been used in the traditional healthcare system from time immemorial, particularly among tribal communities. The World Health Organization (WHO) has listed 20,000 medicinal plants globally[1]; India's contribution[2] is 15–20%. According to the WHO estimate, about 80% of the population in the developing countries depends directly on plants for its medicines[3,4]. In India, about 2000 drugs used are of plant origin[5]. Plant resources are depleting globally at an alarming rate and a number of economically and medicinally important plant species will soon be extinct. In the last few decades over-exploitation of forest resources has led to species loss. As a result, 20–25% of existing plant species in India has become endangered. Medicinal plants are now under great pressure due to their excessive collection or exploitation. The degree of threat to natural populations of medicinal plants

*For correspondence. (e-mail: mishrabp111@yahoo.com)